Journal of Catalysis **202,** 308–318 (2001)
doi:10.1006/jcat.2001.3276, available online at http://www.idealibrary.com on IDEAL®

Vanadium-Containing MCM-41 for Partial Oxidation of Lower Alkanes

Qinghong Zhang, Ye Wang,[1] Yoshihiko Ohishi, Tetsuya Shishido, and Katsuomi Takehira[1]

Department of Applied Chemistry, Faculty of Engineering, Hiroshima University, Kagamiyama 1-4-1, Higashi-hiroshima 739-8527, Japan

Received February 9, 2001; revised May 9, 2001; accepted May 11, 2001; published online August 9, 2001

Vanadium-containing mesoporous molecular sieves synthesized by both template-ion exchange (TIE) and direct hydrothermal (DHT) methods have been studied for partial oxidation of lower alkanes. UV–vis and *in situ* laser Raman spectroscopic studies suggest that the former synthetic method can provide tetrahedrally coordinated vanadium species mainly dispersed on the wall surface of MCM-41, while the latter method leads to vanadium sites mainly incorporated into the framework of MCM-41. H_2-TPR measurements show that the vanadium species in the TIE samples can be reduced at lower temperatures than those in the DHT samples. NH_3-TPD investigations suggest that weak acid sites mainly exist over MCM-41 along with a small amount of medium ones. The introduction of vanadium by the TIE method increased the amount of weak acid sites, while both weak and medium acid sites of MCM-41 are decreased with introducing vanadium up to a certain content by the DHT method. In the oxidations of ethane and propane, the alkane conversions increase remarkably with increasing vanadium content, and moderate selectivities to ethylene and propylene are obtained over the TIE catalysts. The same catalysts, however, are not selective for the oxidative dehydrogenation of isobutane. On the other hand, propylene and isobutene are obtained with high selectivity over the DHT catalysts with vanadium content exceeding 1 wt% in the oxidations of propane and isobutane, respectively. Acrolein and methacrolein can also be formed respectively with considerable selectivity over the DHT catalysts with lower vanadium content. It is likely that the medium acid sites that remained in these samples play roles in the formation of oxygenates through the adsorption of alkenes or allylic intermediates.

Key Words: **V–MCM-41; partial oxidation; oxidative dehydrogenation; lower alkane; acrolein.**

INTRODUCTION

MCM-41, a typical mesoporous molecular sieve, has attracted much attention as catalyst support since it possesses well-ordered channels with controllable uniform pore size of 2–10 nm as well as large surface area. The active component introduced to the channel of MCM-41 could thus be tailored in the nano-order space. Moreover, many heteroatoms could also be incorporated into the wall of MCM-41 to substitute Si^{4+} like the situation in many zeolites, though the framework of MCM-41 is amorphous (1–3). Thus, the isolated active centers as can be seen in metal-substituted aluminosilicate or aluminophosphate molecular sieves can also be generated in the case of MCM-41.

We focus our studies on vanadium-containing MCM-41 because the isolated vanadium site over many supported vanadia catalysts has been suggested to account for the selective oxidation of hydrocarbon (4). Furthermore, vanadium-substituted zeolites such as V–silicalite (5) and VAPO-5 (6, 7) have shown good performance in the oxidative dehydrogenation of propane. Many publications have contributed to the syntheses and characterizations of V–MCM-41 in recent years (8–10), but the studies on its catalytic properties are still scarce and the reports are mainly limited to liquid-phase oxidation using H_2O_2 or *tert*-butyl hydroperoxide (11–13). Only the partial oxidation of methanol (14) and that of methane (15) have been reported so far for gas-phase oxidation using oxygen.

Regarding the synthesis of V–MCM-41, the direct hydrothermal (DHT) method in which a vanadium source such as $VO(C_2O_4)$ or $VO(SO_4)$ is added directly to synthesis gel containing a silicon source and an organic template prior to hydrothermal synthesis has mainly been reported so far (8–14). Conventional impregnation has also been used to prepare vanadium-containing MCM-41 (15, 16). However, this method cannot ensure the introduction of vanadium into the mesopore of MCM-41. Moreover, some contraction of channels seems to occur by the impregnation method. The introduction of vanadium to MCM-41 by a grafting method using an organic vanadium compound has been reported (17, 18). Recently, we found that vanadium could be introduced into the channel of MCM-41 without collapse of the mesoporous structure by a template-ion exchange (TIE) method, viz., by exchanging VO^{2+} ions in the aqueous solution with the template cations comprised in the as-synthesized (uncalcined) MCM-41 (19). This paper is to investigate and compare the catalytic properties of the V–MCM-41 prepared by the TIE and DHT methods in partial oxidation or oxidative dehydrogenation of lower alkanes including ethane, propane, and isobutane.

[1] To whom correspondence should be addressed. Fax: (+81) 824 22 7191. E-mail: yewang@hiroshima-u.ac.jp.

0021-9517/01 $35.00

EXPERIMENTAL

Catalyst Preparation

MCM-41 was prepared by a modified procedure of Beck and co-workers (20). The solution of hexadecyltrimethylammonium bromide ($C_{16}H_{33}(CH_3)_3NBr$) (26.4 g in 110 g of H_2O) was added to the solution of sodium silicate (55 wt% SiO_2, 15.4 g in 80 g of H_2O). The pH of the mixture was adjusted to 11.0 by 4 N HCl. The resulting gel was allowed to stir for 1 h before being transferred to a Teflon bottle and placed in a stainless-steel autoclave. The hydrothermal synthesis was carried out at 120°C for 96 h. The resultant solid was recovered by filtration, washed thoroughly with deionized water (∼20 L) to remove Na^+ and the excess template, and subsequently dried at 40°C in vacuum for 24 h.

For the TIE synthesis of V–MCM-41, 2 g of the as-synthesized MCM-41 containing ca. 50 wt% template was added to a solution of vanadyl oxalate (a certain amount of VOC_2O_4 in 40 g of H_2O), stirred vigorously at ambient temperature for 1 h, and then kept at 80°C for 20 h. The exchanged resultant was filtered, washed thoroughly with deionized water, and then dried at 40°C in vacuum for 24 h. The as-synthesized V–MCM-41 (TIE) was finally calcined by heating from ambient temperature to 550°C at a rate of 1°C/min and kept at 550°C for 6 h in a flow of dry air (1 L/min). If the calcined MCM-41without template was used in the same experiment to replace the as-synthesized MCM-41, less than 10% of the vanadium in the solution remained in MCM-41 after filtration, washing, drying, and calcination. On the other hand, ca. 60–80% of the vanadium was introduced to MCM-41 using the uncalcined MCM-41 (19). These observations support the occurrence of ion exchange between the template cations in the as-synthesized MCM-41 and the VO^{2+} ions in the solution.

For the direct hydrothermal synthesis of V–MCM-41, the solution of vanadyl oxalate (a certain amount of VOC_2O_4 in 40 g of H_2O) was added to the mixture of sodium silicate and $C_{16}H_{33}(CH_3)_3NBr$ solutions before pH adjustment as described in the synthesis of MCM-41. After hydrothermal synthesis at 120°C for 96 h, the product was filtered, washed thoroughly with deionized water, dried at 40°C in vacuum for 24 h, and finally calcined with the same procedure as described for TIE synthesis.

Characterization

XRD was performed using a Rigaku RINT2500VHF diffractometer with Cu *Kα* radiation (45 kV, 450 mA). Small divergent and scattering slits (0.05 mm and 1/6 degrees, respectively) were selected to avoid the high background at low diffraction angle.

The N_2 adsorption isotherm at 77 K was measured using Belsorp 18SP equipment (volumetric). The pore size distribution was determined using the BJH method.

The diffuse reflectance UV–vis spectra were recorded on a Perkin–Elmer UV/VIS/NIR spectrometer (Lambda 900). The powdery sample was loaded in a quartz cell, and the spectra were collected in 230–700 nm with a reference of $BaSO_4$.

In situ laser Raman spectroscopic studies were carried out using a JASCO NR-1800 (OL) spectrometer to obtain information about the coordination of vanadium under the conditions close to those used for reactions. The sample wafer was placed in a high-temperature *in situ* Raman cell made of quartz. The spectra were recorded in O_2 flow at different temperatures.

H_2-temperature-programmed reduction (TPR) was performed using a flow system equipped with a thermal conductivity detector. In a typical experiment, 100 mg of sample was first pretreated in a U-type quartz reactor with a gas flow containing N_2 (20 ml/min) and O_2 (10 ml/min) at 550°C for 1 h and then purged with pure N_2 (30 ml/min). After cooling to 30°C, H_2–N_2 (5% H_2) gas mixture was introduced into the reactor and the temperature was increased to 900°C at a rate of 10°C/min.

NH_3-temperature-programmed desorption (TPD) measurements were carried out on BEL JAPAN TPD-1-AT equipment. After pretreated in a gas flow of He (20 ml/min) and O_2 (10 ml/min) at 550°C, the sample was degassed in vacuum. The adsorption of NH_3 was carried out at 120°C and at a pressure of 2.67 kPa for 1 h, and then the NH_3 that remained in the gas phase was purged by He. TPD was performed in He flow by raising the temperature to 600°C at a rate of 10°C/min. The desorbed NH_3 was detected by a mass spectrometer.

Catalytic Reaction

The partial oxidation reactions were carried out using a conventional fixed-bed flow reactor: 0.2 g of catalyst, which had been pelletized and sieved to 250–417 μm, was loaded into a U-type reactor made of quartz tube and treated in a gas flow containing N_2 (10 ml/min) and O_2 (3 ml/min) at 550°C for 1 h before reaction. The reaction was started by introducing a gas mixture of N_2 (10 ml/min), O_2 (3 ml/min), alkane (6 ml/min), and He (31 ml/min) to the reactor. N_2 was used as the internal standard for calculating the conversions of O_2 and alkane, while He was used for dilution to control the partial pressures of reactants. The products were analyzed by on-line gas chromatographs. The alkane conversion was also calculated from the concentrations of products and the remained alkanes, and carbon balance was evaluated. Generally, carbon balance was better than 95%.

Blank runs were also carried out with an empty reactor under above reaction conditions. For C_2H_6 oxidation, no reaction occurred at $\leq$550°C and the conversion of C_2H_6 was 1.2% at 600°C. In the cases of oxidation of C_3H_8 and i-C_4H_{10}, the conversions of C_3H_8 and i-C_4H_{10} were

not detectable at ≤550 and 500°C, respectively. Catalytic reactions were thus carried out using the conditions under which the gas-phase reactions could be neglected.

RESULTS AND DISCUSSION

Properties of Catalysts

Figure 1 shows XRD patterns of the samples prepared by both TIE and DHT methods with different Si/V ratios. The Si/V ratio shown here was determined from ICP measurements. For TIE samples (Fig. 1A), four diffraction peaks ascribed to (100), (110), (200), and (210) of MCM-41 were all observed, and the peak intensity was almost kept with increasing vanadium content to a Si/V ratio of 23, indicating no de-organization at long range of the mesoporous structure of MCM-41 during TIE synthesis. For DHT samples (Fig. 1B), the peak of (210) at 2θ of ca. 6° was not clearly observed. This phenomenon was also observed previously and was suggested to relate to the incorporation of vanadium to the wall of MCM-41 (9). Concerning the shift of peak position after introducing vanadium, Sayari and co-workers (8) reported a slight shift of (100) to lower diffraction angle, in other words, a slight increase in *d* spacing. However, the results from the groups of Kevan and co-workers (9) and Haller and co-workers (10) showed an obvious decrease in *d* spacing after introducing vanadium to MCM-41. Here, no definite tendency in peak shift was observed with increasing vanadium content. As vanadium content increased up to a Si/V ratio of 23 [Fig. 1B (g)], only the peak of (100) was detectable, indicating the decrease in structural regularity.

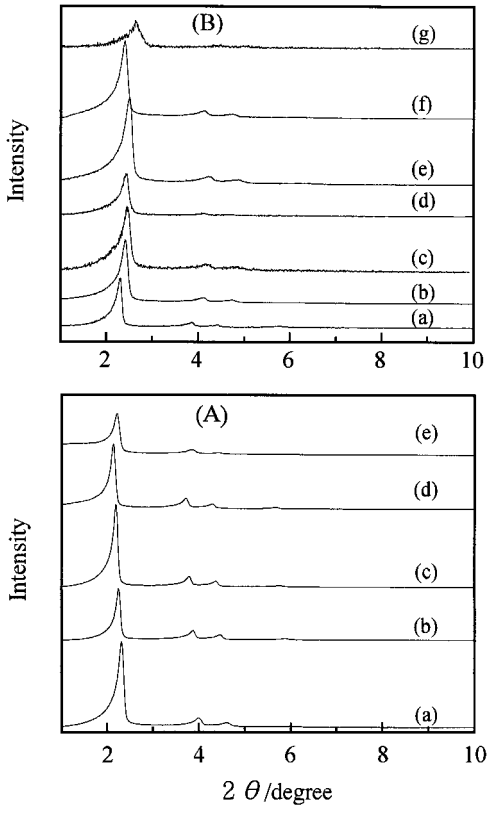

FIG. 1. XRD patterns of V–MCM-41 by TIE and DHT methods. (A) TIE method, (a) MCM-41, (b) Si/V = 83, (c) Si/V = 47, (d) Si/V = 23, (e) Si/V = 12; (B) DHT method, (a) MCM-41, (b) Si/V = 543, (c) Si/V = 210, (d) Si/V = 120, (e) Si/V = 87, (f) Si/V = 40, (g) Si/V = 23.

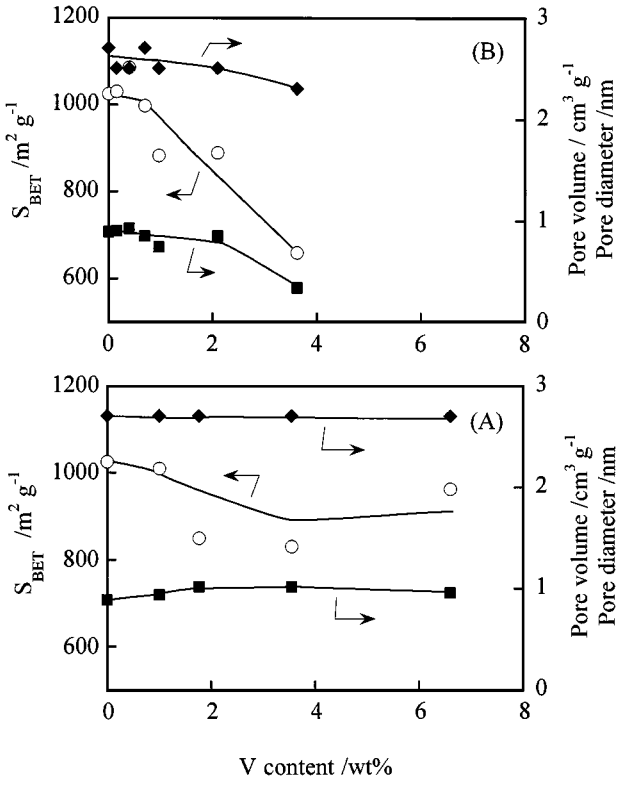

FIG. 2. Results obtained from N_2 adsorption isotherms of the TIE (A) and DHT (B) samples at 77 K. (○) BET surface area, (■) pore volume, (◆) pore diameter.

The BET surface area, pore volume, and pore diameter as functions of vanadium content are shown in Fig. 2. The increase in vanadium content slightly decreased the surface area but did not significantly alter the pore volume and pore diameter of TIE sample. However, the surface area and the pore volume of DHT sample dropped remarkably as vanadium content increased up to 3.6 wt% (Si/V = 23). The shrinkage of pore diameter was also observed at the same time. These observations agreed well with the XRD results shown in Fig. 1B, which indicated a de-organization at long range as vanadium content increased to a Si/V ratio of 23. Thus, the amount of vanadium introduced to MCM-41 by the DHT method without destroying its mesoporous structure was less than that by the TIE method.

Figure 3 shows the diffuse reflectance UV-vis spectra of V-MCM-41. For the as-synthesized samples [Figs. 3A,

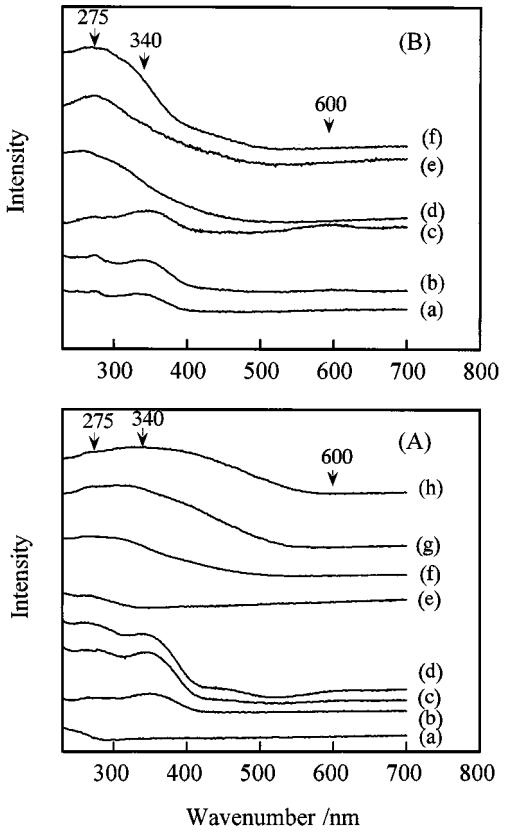

FIG. 3. Diffuse reflectance UV–vis spectra of V–MCM-41. (A) TIE samples, (a) MCM-41 as-synthesized, (b) Si/V = 83, as-synthesized, (c) Si/V = 47 as-synthesized, (d) Si/V = 23 as-synthesized, (e) MCM-41 calcined, (f) Si/V = 83 calcined, (g) Si/V = 47 calcined, (h) Si/V = 23 calcined; (B) DHT samples, (a) Si/V = 210 as-synthesized, (b) Si/V = 87 as-synthesized, (c) Si/V = 23 as-synthesized, (d) Si/V = 210 calcined, (e) Si/V = 87 calcined, (f) Si/V = 23 calcined.

(b)–(d), and 3B, (a)–(c)], both TIE and DHT methods exhibited UV–vis absorption bands at ca. 275 and 340 nm, both of which could be assigned to the low-energy charge-transfer transitions between tetrahedral oxygen ligands and the V^{5+} center. A weak band near 600 nm, which arose from the d–d transition of VO^{2+} cation, was also observed for the samples with high vanadium content. These results suggest that some tetrahedrally coordinated vanadium species already exist in the as-synthesized samples. Since the sensitivity of the band at 600 nm of VO^{2+} is much lower than that of the band at 275 or 340 nm (21), a large part of VO^{2+} may still exist though they could not be observed with UV–vis spectroscopy.

After calcination at 550°C, the absorption bands at 275 and 340 nm overlapped and the spectra became broad, particularly for the TIE samples as shown in the figure. The samples with low vanadium content showed the main peak at 275 nm, and the component at 340 nm increased with increasing vanadium content. The component at 340 nm became dominant for the TIE samples as the vanadium content exceeded 1.8 wt% (Si/V = 47), while that at 275 nm was still the main component for the DHT sample even with vanadium content of 3.6 wt% (Si/V = 23). Combining the results of ESR and ^{51}V NMR, Kevan and coworkers (9) suggested that the UV band at 275 nm observed for the calcined V–MCM-41 corresponded to the vanadium incorporated inside the framework of MCM-41 while that at 340 nm corresponded to the vanadium on its wall. Thus, the results obtained here suggest that the vanadium species mainly exist on the wall surface in the TIE samples, while a large part of them are incorporated inside the framework of MCM-41 in the DHT samples. Furthermore, the contribution of the square pyramidal (415 nm) and octahedral (450 nm) type vanadium species became considerable in the TIE samples with high vanadium content. Such species were probably formed due to the hydration of the surface tetrahedral vanadium under ambient conditions (9).

In our preceding paper (19), we reported that the terminal V=O bond of monomer VO_4 tetrahedron dispersed on MCM-41 was observed by laser Raman spectroscopy (Raman shift at ca. 1035 cm^{-1}) for the TIE samples, while such terminal V=O was almost not detectable for the DHT samples. However, because those measurements were carried out under ambient conditions, a large part of the vanadium may be hydrated as indicated by the results of UV–vis experiments. We thus carried out *in situ* Raman measurements in O_2 flow at different temperatures. Figure 4 shows the spectra of TIE (Si/V = 47) and DHT (Si/V = 40) samples with a similar vanadium content. In the case of TIE sample (Fig. 4A), the peak at 1030 cm^{-1} was clearly observed, even at 23°C, and the intensity of this peak increased remarkably with temperature, indicating the increase in the concentration of terminal V=O. Probably, the removal of H_2O or OH, which was coordinated to vanadium under ambient conditions, formed mainly monomer VO_4 tetrahedron with terminal V=O in the presence of O_2 at high temperature. A weak peak at ca. 970 cm^{-1}, which could be assigned to Si–O–Si stretching vibration (22), also appeared as the temperature rose. The peak ascribed to V–O–V stretching was observed at ca. 920 cm^{-1}, but it was very weak, even at high temperature, suggesting that the oligomeric VO_x cluster was only minor, even at reaction temperature over the TIE sample. For the DHT sample (Fig. 4B), the peak at 1030 cm^{-1} could almost not be observed at room temperature, but it appeared and gradually increased as the temperature was raised. This observation indicates that the terminal V=O also exists on the surface of the DHT sample under temperatures close to those used for reactions in the presence of O_2. However, the intensity of this peak was much lower (ca. 1/6 at 400°C and 1/4 at 480°C) as compared with that for the TIE sample, suggesting a lower concentration of the terminal V=O on the surface of the DHT sample. This may be an indication

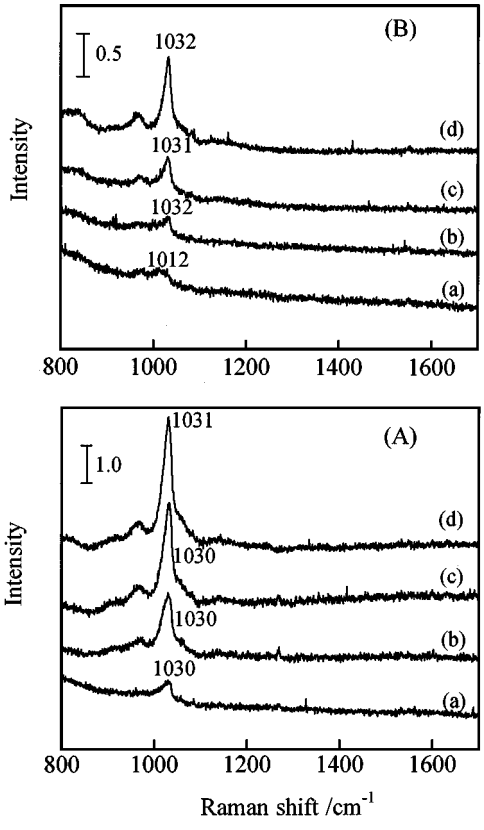

FIG. 4. *In situ* laser Raman spectra of V–MCM-41 in O_2 flow (50 ml/min) at different temperatures. (A) TIE sample with Si/V ratio of 47, (a) 23°C, (b) 291°C, (c) 400°C, (d) 480°C; (B) DHT sample with Si/V ratio of 40, (a) 23°C, (b) 300°C, (c) 400°C, (d) 483°C.

that a large part of vanadium was incorporated into the framework. The fact that the peak at 920 cm^{-1} belonging to V–O–V has not been observed for this sample suggests that vanadium is highly isolated.

Figure 5 shows H_2-TPR profiles. Both TIE and DHT samples showed a single reduction peak, which was completely different from those for V_2O_5. For TIE samples, the peak temperature changed from 518 to 525°C with increasing vanadium content from 1.0 wt% (Si/V = 83) to 3.6 wt% (Si/V = 23). The reduction peaks were at 548 and 579°C for the DHT samples with similar vanadium contents to the TIE samples. Therefore, the vanadium species in TIE samples could be reduced more easily as compared with that in DHT samples. Wachs and co-workers (22) have reported that the reduction peak for surface vanadium oxide species highly dispersed on a silica support (V content, 1 wt%) appears at ca. 525°C and that for vanadium in V-substituted silicalite (V content, 1.5 wt%) is at ca. 550°C. These two peak temperatures are almost the same as those observed here for the TIE and DHT samples (Fig. 5), respectively. This suggests that the coordination environments of vanadium species in TIE and DHT samples resemble those in silica-supported highly dispersed vanadium oxide and V-substituted silicalite, respectively. Such a result is consistent with the conclusion from UV–vis and laser Raman spectroscopic measurements described above.

The acidic properties of V–MCM-41 prepared by TIE and DHT methods were investigated by NH_3-TPD and the results were shown in Fig. 6. MCM-41, without vanadium, showed a main peak at 502 K and a broad shoulder at 710–730 K, suggesting that weak acid sites were dominant on MCM-41, but some with medium strength also existed. Recently, FSM-16, another type of pure siliceous mesoporous material, has been found to possess acid sites (H_0 = ca. −3.0 to −5.6) stronger than amorphous silica (H_0 = ca. +3.0 to +4.8), and the nature of such acid sites is suggested to be perturbed silanol groups (23, 24). Although we still do not know the natures of the acid sites in pure siliceous MCM-41 at this moment, we speculate that the acid sites with medium strength might also arise from the silanol groups on defective sites. Figure 6A showed that the peak intensity for weak acid sites was remarkably increased with introducing vanadium by the TIE method, and the peak position slightly shifted to lower temperature at the same time. The peak at 710–730 K ascribed to the acid sites with medium strength, however, vanished simultaneously, probably due to the covering of such acid sites by vanadium species. On the other hand, these medium acid sites remained after introducing a small amount of vanadium by the DHT method, but both the medium and the weak acid sites became attenuated as the vanadium content increased above 0.7 wt% (Si/V = 120) and the shift of peak position to lower temperature was also observed at the same time. Lim and Haller (14) have observed the increase in the amount of weak Lewis acid by increasing

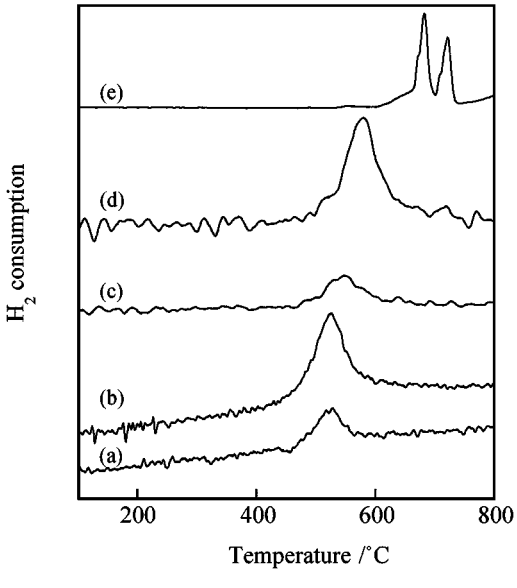

FIG. 5. H_2-TPR profiles of V–MCM-41. (a) TIE Si/V = 83, (b) TIE Si/V = 23, (c) DHT Si/V = 87, (d) DHT Si/V = 23, (e) V_2O_2 (5 mg).

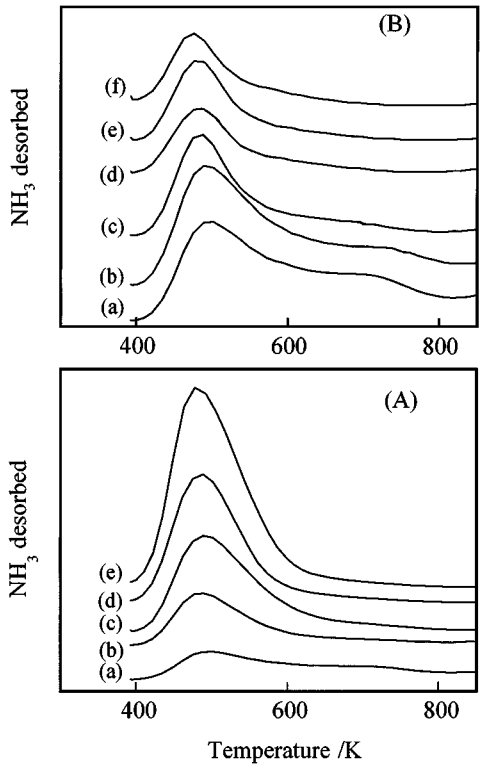

FIG. 6. NH_3-TPD profiles of V–MCM-41. (A) TIE samples, (a) MCM-41, (b) Si/V = 83, (c) Si/V = 47, (d) Si/V = 23, (e) Si/V = 12; (B) DHT samples, (a) MCM-41, (b) Si/V = 210, (c) Si/V = 120, (d) Si/V = 87, (e) Si/V = 40, (f) Si/V = 23. Note: the scales of the vertical axes for (A) and (B) are different.

vanadium content in V–MCM-41 and ascribed such weak Lewis acid sites to isolated vanadium sites tetrahedrally coordinated with oxygen. As described above, in our case, the tetrahedral vanadium species were mainly dispersed on the wall surface of MCM-41 in the TIE samples. Thus, the increase in weak acid sites with increasing vanadium content in TIE samples could probably be due to the increase in the concentration of surface-isolated tetrahedral vanadium species. On the other hand, in the case of DHT samples, a large part of vanadium atoms were incorporated into the framework, and the surface concentration of vanadium was limited. Moreover, the surface area was also decreased to some extent by increasing vanadium to a high content. These probably led to the slight decrease in the weak acid sites with increasing vanadium content as shown in Fig. 6B.

Catalytic Oxidation of Ethane

Figure 7 compares the results obtained from the oxidation of C_2H_6 using TIE and DHT samples at 550°C. For TIE samples (Fig. 7A), C_2H_6 conversion increased almost linearly with increasing vanadium content up to 3.6 wt% (Si/V = 23), and a further increase in vanadium content did not remarkably affect C_2H_6 conversion. C_2H_4 selectivity slightly decreased with introducing vanadium to MCM-41 but did not change with vanadium content. In other words, the increase in vanadium content increased C_2H_6 conversion but did not significantly enhance the consecutive oxidation of C_2H_4 to CO and CO_2.

For the oxidation of C_2H_6 over DHT samples, as shown in Fig. 7B, the incorporation of vanadium also enhanced the reaction, but the increase in C_2H_6 conversion was decelerated as vanadium content exceeded 0.7 wt% (Si/V = 120). Furthermore, C_2H_6 conversion dropped as vanadium content increased from 2 to 3.6 wt%. C_2H_4 selectivity showed a tendency to decrease with increasing vanadium content. Thus, the DHT sample with high vanadium content is not selective for the oxidative dehydrogenation of C_2H_6.

Figure 8 shows the change of catalytic performance with reaction temperature over the TIE and DHT samples with the same vanadium content of 3.6 wt% (Si/V = 23). The TIE sample gave higher C_2H_6 conversion than the DHT sample in the whole temperature region investigated. The activation energies calculated for the TIE and DHT samples were 120 and 95 kJ mol^{-1}, respectively. C_2H_4 selectivity decreased with increasing temperature over the TIE sample probably due to the consecutive oxidation. The increase

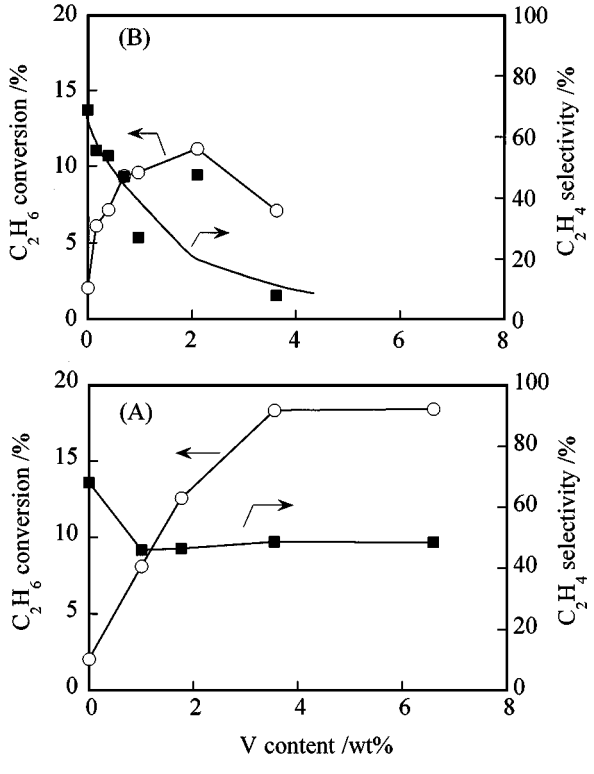

FIG. 7. Results for catalytic oxidation of C_2H_6 over V–MCM-41 by TIE (A) and DHT (B) methods. (○) C_2H_6 conversion, (■) C_2H_4 selectivity. Conditions: $W = 0.2$ g, $T = 550$°C, $F = 50$ ml/min, $P(C_2H_6) = 12.2$ kPa, $P(O_2) = 6.1$ kPa.

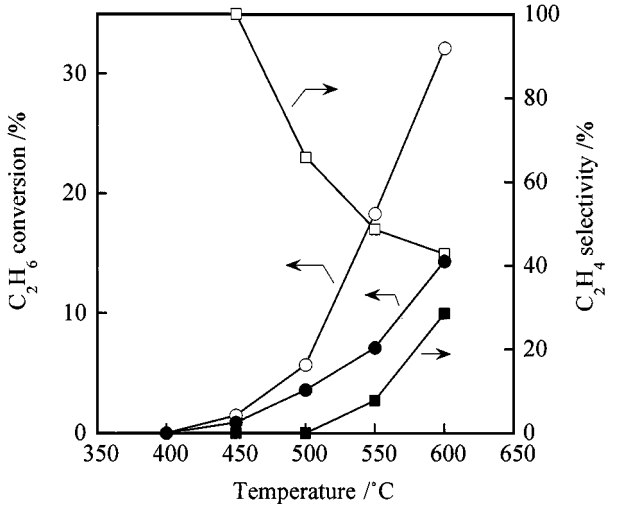

FIG. 8. Effect of reaction temperature on catalytic oxidation of C_2H_6 over V–MCM-41 with a Si/V ratio of 23. (○) TIE C_2H_6 conversion, (□) TIE C_2H_4 selectivity, (●) DHT C_2H_6 conversion, (■) DHT C_2H_4 selectivity. Conditions: $W = 0.2$ g, $F = 50$ ml/min, $P(C_2H_6) = 12.2$ kPa, $P(O_2) = 6.1$ kPa.

in C_2H_4 selectivity with increasing temperature at $\geq$550°C, however, was observed over the DHT sample. Probably, the contribution of gas-phase radical reactions, which may produce C_2H_4, cannot be neglected at such a high temperature.

Catalytic Oxidation of Propane

Figure 9 shows the results of C_3H_8 oxidation over TIE and DHT samples with different vanadium content. The oxidation of C_3H_8 over pure siliceous MCM-41 produced mainly CO_2 along with a small amount of acrolein at 500°C. C_3H_8 conversion increased remarkably with increasing vanadium content over TIE samples (Fig. 9A). C_3H_6 selectivity also increased with increasing vanadium content up to 1.8 wt% (Si/V = 47) and did not significantly change with a further increase in vanadium content. In the case of DHT samples (Fig. 9B), the introduction of vanadium also enhanced the reaction, but C_3H_8 conversion showed a tendency to decrease as vanadium content exceeded 1.0 wt% (Si/V = 87). C_3H_6 selectivity increased sharply with increasing vanadium content up to 1.0 wt% and then was held at a high level of ca. 70%. Not only C_3H_6 but acrolein was also formed over DHT samples. The selectivity to acrolein was the highest over the sample with vanadium content of 0.4–0.7 wt% (Si/V = 210–120) at 500°C. Further increasing in vanadium content decreased its selectivity.

To compare the selectivity to C_3H_6 and acrolein over TIE and DHT samples at a similar C_3H_8 conversion level, the catalytic results over DHT samples at 550°C were shown in Fig. 9C. At such a temperature, C_3H_8 conversion increased to >15% with increasing vanadium content up to 0.7 wt% (Si/V = 120), and simultaneously, C_3H_6 selectivity increased near 60%. As compared with the results for TIE samples (Fig. 9A), it is apparent that higher C_3H_6 selectivity could be achieved over DHT samples at a similar C_3H_8 conversion level. Furthermore, acrolein with a selectivity of ca. 20% and yield of ca. 3% was obtained over the DHT sample with a vanadium content of 0.7 wt% (Si/V = 120), while acrolein was nearly not formed over TIE samples. It should be mentioned that C_3H_6 yield over the DHT samples with vanadium content $\geq$1 wt% was comparable to the best one achieved over V–silicalite and VAPO-5 zeolites (5–7). However, the formation of a considerable amount of acrolein has never been reported over V-containing zeolites or silica-supported vanadia catalysts. Thus, V–MCM-41 synthesized by the DHT method is unique for the partial oxidation of C_3H_8 to acrolein.

To obtain further information about the formations of C_3H_6 and acrolein, the effects of reaction conditions

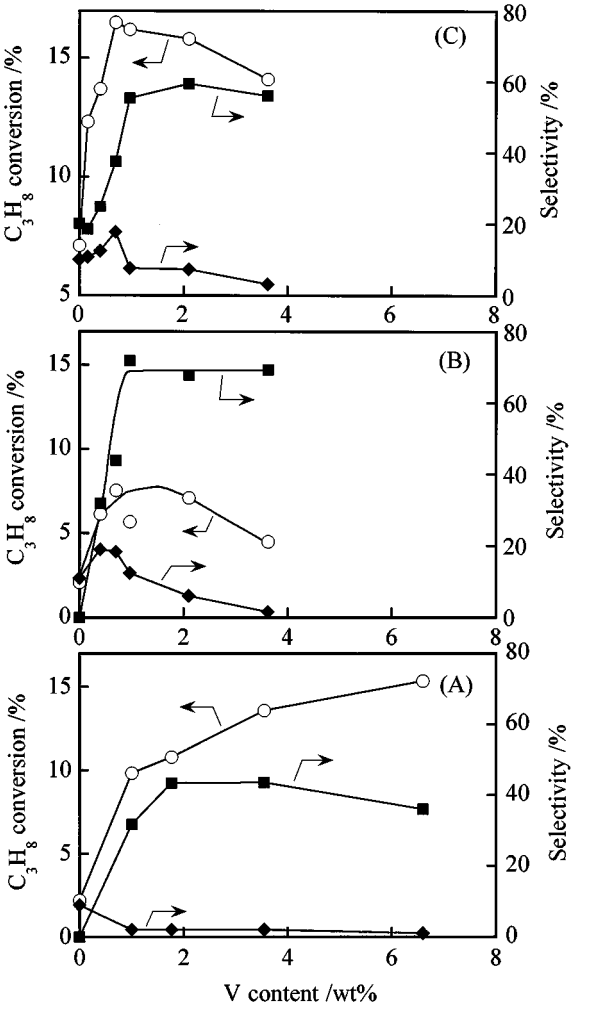

FIG. 9. Results for catalytic oxidation of C_3H_8 over V–MCM-41 by TIE (A) and DHT (B, C) methods. (○) C_3H_8 conversion, (■) C_3H_6 selectivity, (◆) acrolein selectivity. Conditions: $W = 0.2$ g, $T = 500$°C (for A and B) and 550°C (for C), $F = 50$ ml/min, $P(C_3H_8) = 12.2$ kPa, $P(O_2) = 6.1$ kPa.

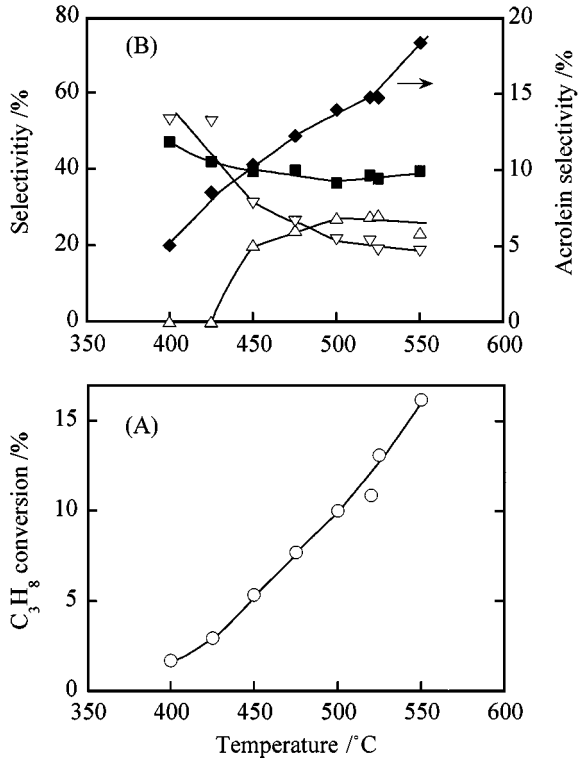

FIG. 10. Effect of reaction temperature on catalytic oxidation of C_3H_8 over V–MCM-41 by the DHT method (V content 0.7 wt%, Si/V = 120). (A) (○) C_3H_8 conversion; (B) (■) C_3H_6 selectivity, (◆) acrolein selectivity, (△) CO selectivity, (▽) CO_2 selectivity. Conditions: $W = 0.2$ g, $F =$ 50 ml/min, $P(C_3H_8) = 12.2$ kPa, $P(O_2) = 6.1$ kPa.

were investigated over the catalyst (V content 0.7 wt%, Si/V = 120) with the highest acrolein selectivity. Figure 10 shows the influence of reaction temperature on C_3H_8 conversion and product selectivities. C_3H_8 conversion increased with reaction temperature and the activation energy for C_3H_8 conversion was calculated to be 67 kJ mol^{-1}. The increase in temperature increased the selectivity to acrolein and decreased that to CO_2. C_3H_6 selectivity slightly decreased by increasing the temperature to 500°C. CO began to be formed at >425°C.

Figure 11 shows the effect of partial pressure of O_2 on catalytic performances at 520°C and constant C_3H_8 pressure of 12.2 kPa. C_3H_8 conversion increased with increasing O_2 pressure, and the calculation from a plot of the logarithm of $r(C_3H_8)$ versus the logarithm of $P(O_2)$ indicated that the reaction order for O_2 was 0.60 ± 0.05. At low O_2 pressure, C_3H_6 and acrolein were dominant products. The sum of the selectivities to C_3H_6 and acrolein reached 95 and 87% with C_3H_8 conversion of 3.0 and 4.4% at O_2 pressures of 1.0 and 2.0 kPa, respectively. To our knowledge, these results are outstanding among all the reported catalysts for partial oxidation of C_3H_8. C_3H_6 selectivity decreased first sharply in a low O_2 pressure range and then gradually with increasing O_2 pressure. Acrolein selectivity increased as the O_2 pressure increased from 1.0 to 2.0 kPa, but decreased with a further increase in O_2 pressure.

As shown in Fig. 12, at a constant O_2 partial pressure, the increase in C_3H_8 pressure did not significantly change C_3H_8 conversion, and the C_3H_8 conversion rate increased almost linearly with C_3H_8 pressure except for the point of 30 kPa at which the O_2 conversion exceeded 50% (Fig. 12A). This observation suggests a first-order dependence of C_3H_8 conversion rate on the partial pressure of C_3H_8. At low C_3H_8 pressure, CO_2 was mainly formed along with a small amount of acrolein (Fig. 12B). The increase in C_3H_8 pressure decreased the selectivity to CO_2 and increased those to acrolein and C_3H_6.

The results described above suggest that acrolein is produced through the oxidation of C_3H_6 or allylic intermediate adsorbed on a catalyst surface since the increase in O_2 pressure increased the selectivity to acrolein but decreased that to C_3H_6 at very low O_2 pressure (Fig. 11B). At low temperatures, CO_2 was formed as a main product (Fig. 10B) probably due to further oxidation of acrolein to CO_2 on a catalyst surface. The increase in temperature may enhance the desorption of acrolein or C_3H_6 and thus increase the selectivity to acrolein (Fig. 10B). Since CO began to appear at high temperatures (Fig. 10B) or high C_3H_8 conversion

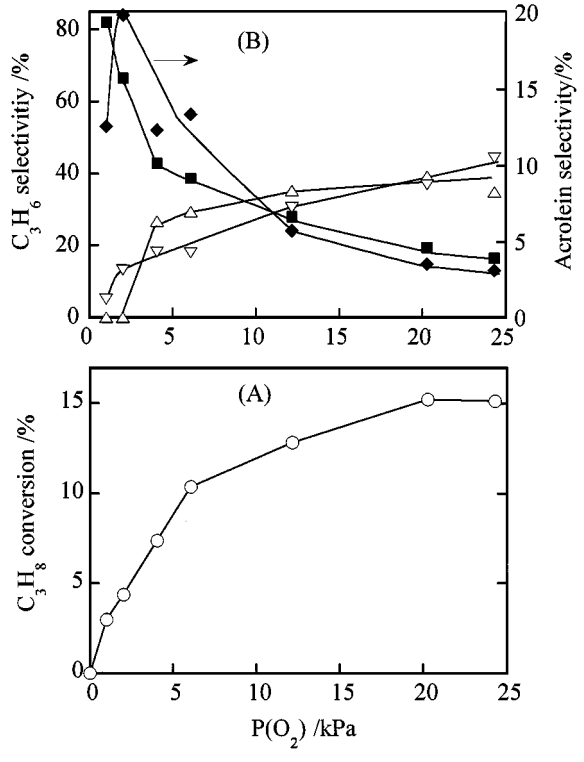

FIG. 11. Effect of partial pressure of O_2 on catalytic oxidation of C_3H_8 over V–MCM-41 by the DHT method (V content 0.7 wt%, Si/V = 120). (A) (○) C_3H_8 conversion; (B) (■) C_3H_6 selectivity, (◆) acrolein selectivity, (△) CO selectivity, (▽) CO_2 selectivity. Conditions: $W = 0.2$ g, $T = 520$°C, $F = 50$ ml/min, $P(C_3H_8) = 12.2$ kPa.

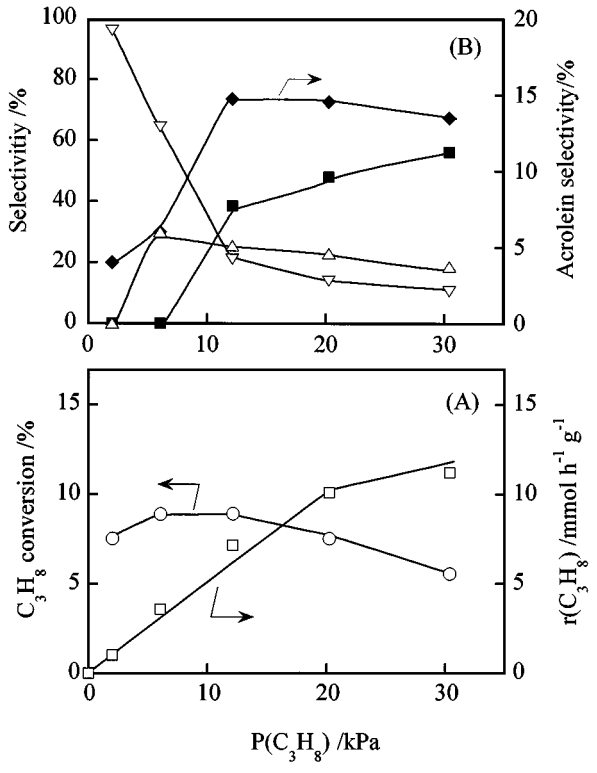

FIG. 12. Effect of partial pressure of C_3H_8 on catalytic oxidation of C_3H_8 over V–MCM-41 by the DHT method (V content 0.7 wt%, Si/V = 120). (A) (○) C_3H_8 conversion, (□) C_3H_8 conversion rate; (B) (■) C_3H_6 selectivity, (◆) acrolein selectivity, (△) CO selectivity, (▽) CO_2 selectivity. Conditions: $W = 0.2$ g, $T = 520$°C, $F = 50$ ml/min, $P(O_2) = 6.1$ kPa.

(Fig. 11B), it may be formed through the consecutive oxidation of both C_3H_6 and acrolein in gas phase.

Catalytic Oxidation of Isobutane

Figure 13 compares the catalytic performances of TIE and DHT samples in the oxidation of i-C_4H_{10} at 500°C. MCM-41 without vanadium gave i-C_4H_{10} conversion of 5.5%. For TIE samples, i-C_4H_{10} conversion increased with increasing vanadium content and was saturated as vanadium content exceeded 2 wt% due to the complete consumption of O_2. The main products were CO and CO_2, and the selectivity to partial oxidation products, i.e., i-C_4H_8 and methacrolein, was lower than 15%. Over DHT samples, i-C_4H_{10} conversion increased more remarkably with increasing vanadium content up to 2 wt%, although a further increase in vanadium content decreased the conversion. Moreover, i-C_4H_8 was formed with selectivity of ca. 50% over the DHT samples as the vanadium content exceeded 1 wt%, which was much higher than those over the TIE samples. Interestingly, similar to C_3H_8 oxidation, methacrolein, the product of allylic oxidation, was also formed with moderate selectivity (ca. 20%) over DHT samples with lower vanadium content.

Comparison of the Reactions over TIE and DHT Catalysts

(a) TIE catalysts. The tendencies of the change of alkane conversion versus vanadium content over these samples are very similar (Figs. 7A, 9A, and 13A); the conversions are all increased with vanadium content and saturated due to the consumption of O_2 at high vanadium content. Further comparisons with the DHT catalysts tend to suggest that the TIE catalysts show higher activity (higher alkane conversion or O_2 conversion) under the same reaction conditions. This is probably also related to the redox properties of vanadium species in these two kinds of catalysts. As described in Fig. 5, the vanadium species in TIE catalysts could be reduced more easily.

In the cases of C_2H_6 and C_3H_8 oxidation, moderate selectivities to their alkenes, viz., approximately 50 and 40% to C_2H_4 and C_3H_6, respectively, were obtained over the TIE samples as vanadium content exceeded 1 wt%, and these selectivities were almost held with a further increase in vanadium content. This must be caused by the high dispersion of vanadium species on the wall of MCM-41 in these samples, which has been indicated by the results of diffuse reflectance UV–vis (Fig. 3), laser Raman (Fig. 4), and H_2-TPR (Fig. 5) studies. However, it should be noted that these TIE samples showed very low selectivity in the oxidative dehydrogenation of i-C_4H_{10} to i-C_4H_8. This must be due to

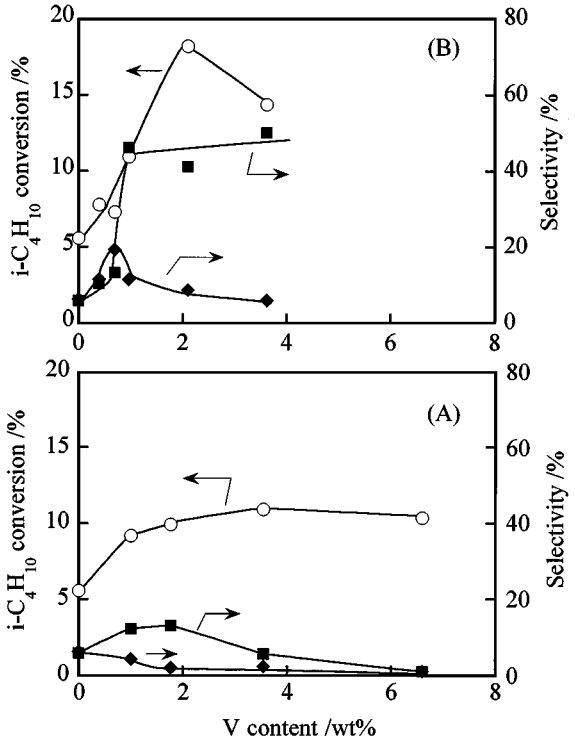

FIG. 13. Results for catalytic oxidation of i-C_4H_{10} over V–MCM-41 by TIE (A) and DHT (B) methods. (○) i-C_4H_{10} conversion, (■) i-C_4H_{10} selectivity, (◆) methacrolein selectivity. Conditions: $W = 0.2$ g, $T = 500$°C, $F = 50$ ml/min, P(i-C_4H_{10}) = 12.2 kPa, $P(O_2) = 6.1$ kPa.

the higher reactivity of i-C_4H_{10} as compared with that of C_2H_6 and C_3H_8. It is likely that not only consecutive oxidation of i-C_4H_8 but also the direct oxidation of i-C_4H_{10} to CO and CO_2 occurs over the TIE catalysts since high selectivity cannot be obtained over these catalysts, even at very low i-C_4H_{10} conversion. Thus, weaker or more isolated catalytic sites, as in the case of DHT catalysts, are needed to achieve higher selectivity to i-C_4H_8.

(b) DHT catalysts. The variations of alkane conversion as a function of vanadium content over these samples also resembled each other in essence (Figs. 7B, 9B, and 13B). The decrease in conversion was observed in all cases as the vanadium content exceeded a certain amount. The drop in specific surface area (Fig. 2) and the decrease in the regularity of mesoporous structure with vanadium content exceeding 2 wt% (Figs. 1 and 2) may be two of the reasons. Furthermore, since a large part of vanadium atoms were incorporated inside the framework of MCM-41 in DHT samples as indicated by UV–vis, laser Raman, and TPR studies, it can be speculated that only those that remained on the surface or accessible to reactants can work as active sites in the reaction. This may be the other reason why the conversions of C_2H_6 and C_3H_8 did not increase remarkably with increasing vanadium content, as in the case of TIE catalysts.

It should be stressed that the DHT samples showed very different catalytic properties toward C_2H_6 and C_3H_8 or i-C_4H_{10}. As shown in Fig. 7B, the DHT samples with high vanadium content are not appropriate for oxidative dehydrogenation of C_2H_6 to C_2H_4, but they are selective for the formations of C_3H_6 and i-C_4H_8 in the oxidations of C_3H_8 and i-C_4H_{10} (Figs. 9B, 9C, and 13B). Although we cannot provide an unambiguous explanation at this moment, it seems that this may arise from the difference in the oxidation of C_2H_6 and that of C_3H_8 or i-C_4H_{10}. Generally, the activation of C_2H_6 requires more active catalytic species than that for C_3H_8 or i-C_4H_{10}. Thus, only the isolation of vanadium sites from each other may not be necessary to obtain high C_2H_4 selectivity. López Nieto and co-workers (25) reported that the selectivity to C_2H_4 was also related to the presence of acid sites for the oxidation of C_2H_6 over MgVAPO-5. The lower acidity of the DHT catalysts with high vanadium content (Fig. 6B) may be related to their lower C_2H_4 selectivity.

For the oxidation of C_3H_8 or i-C_4H_{10}, higher selectivity to C_3H_6 or i-C_4H_8 was obtained over the DHT samples, probably due to the higher isolation of vanadium sites in these samples. In the case of C_3H_8 oxidation, C_3H_6 selectivity of 60% could be obtained at C_3H_8 conversion of 16% over the DHT catalyst with a Si/V ratio of 40 at 550°C. At 532°C, a V-containing zeolite, V–silicalite-1 (VS-1), gave C_3H_8 conversion of ca. 22% and C_3H_6 selectivity of ca. 45% (5). Thus, the best yield of C_3H_6 over the V–MCM–41 was comparable to that obtained over the VS-1. However, the rate of C_3H_6 formation was ca. 8 mmol g^{-1} h^{-1} over the V–MCM-41, which was higher than that over the VS-1 (ca. 1 mmol g^{-1} h^{-1}).

Besides alkenes, the products of allylic oxidation, i.e., acrolein and methacrolein, were also formed respectively with considerable selectivity over the DHT samples with low vanadium content. It should be noted that oxygenate was not formed in the oxidation of C_2H_6. This could be explained by assuming that the oxygenate formed in the oxidation of C_3H_8 and of i-C_4H_{10} results from the allylic oxidation of the alkenes or allylic intermediates since no such allylic oxidation can occur in the case of C_2H_4. The results obtained by changing reaction conditions in C_3H_8 oxidation (Figs. 10–12) also support that acrolein is produced from the allylic oxidation of C_3H_6 or allylic intermediate on a catalyst surface.

On the other hand, it should be mentioned that the formation of acrolein was not observed over V-substituted zeolites such as VS-1, although they were also effective in the oxidative dehydrogenation of C_3H_8 to C_3H_6. Thus, the features of MCM-41, such as pore structure or specific acidic properties, may have relations with the reaction. The acid sites with medium strength which remained over the DHT samples with low vanadium content (Fig. 6B) and the specific pore structure of these samples might contribute to the adsorption of C_3H_6 or i-C_4H_8 intermediate and thus the formation of acrolein or methacrolein. The disappearance of such acid sites with further increasing vanadium content decreased the selectivity to acrolein and increased that to C_3H_6.

CONCLUSIONS

The vanadium species introduced by the template-ion-exchange method were mainly dispersed on the wall of MCM-41 in the state of monomeric tetrahedral coordination, while the direct hydrothermal method led to vanadium sites mainly incorporated inside the framework of MCM-41. During the oxidations of C_2H_6 and C_3H_8, the conversion of alkane increased remarkably with increasing vanadium content over TIE catalysts and moderate selectivities to C_2H_4 and C_3H_6 (ca. 50 and 40% at 550 and 500°C, respectively) were almost held simultaneously. TIE catalysts, however, were not selective for the oxidation of i-C_4H_{10} to i-C_4H_8. The conversion of C_2H_6, C_3H_8, or i-C_4H_{10} also increased with introduction of vanadium to MCM-41 by the DHT method, but the decrease in conversion was observed as the vanadium content became high. The DHT catalysts showed poor selectivity for the oxidative dehydrogenation of C_2H_6 to C_2H_4. However, high selectivities to C_3H_6 and i-C_4H_8 (ca. 60 and 50% with conversion >15% at 550°C, respectively) were obtained in the oxidations of C_3H_8 and i-C_4H_{10} over the DHT catalysts with vanadium content exceeding 1.0 wt%. Besides C_3H_6 and i-C_4H_8, acrolein and methacrolein were also achieved over the DHT catalysts

with lower vanadium content in the same reactions. The highest yield of acrolein obtained was 3% with selectivity approaching 20%. At low O_2 pressures (1.0 and 2.0 kPa), the sum of the selectivities to C_3H_6 and acrolein could reach 95 and 87% with C_3H_8 conversions of 3.0 and 4.4%, respectively. Acrolein is probably formed by the allylic oxidation of C_3H_6 or allylic intermediate, and the acid sites with medium strength in the catalyst are suggested to play roles in the adsorption of C_3H_6 or allylic intermediate and thus contribute to the formation of acrolein.

REFERENCES

1. Ying, J. Y., Mehnert, C. P., and Wong, M. S., *Angew. Chem. Int. Ed.* **38**, 56 (1999).
2. Biz, S., and Occelli, M. L., *Catal. Rev.-Sci. Eng.* **40**, 329 (1998).
3. Corma, A., *Chem. Rev.* **97**, 2373 (1997).
4. Mamedov, E. A., and Cortés Corberán, V., *Appl. Catal. A* **127**, 1 (1995).
5. Centi, G., and Trifiro, F., *Appl. Catal. A* **143**, 3 (1996).
6. Blasco, T., Concepción, P., López Nieto, J. M., and Pérez-Pariente, J., *J. Catal.* **152**, 1 (1995).
7. Okamoto, M., Luo, L., Labinger, J. A., and Davis, M. E., *J. Catal.* **192**, 128 (2000).
8. Reddy, K. M., Moudrakovski, I., and Sayari, A., *J. Chem. Soc. Chem. Commun.* 1059 (1994).
9. Luan, Z., Xu, J., He, H., Klinoswki, J., and Kevan, L., *J. Phys. Chem.* **100**, 19595 (1996).
10. Wei, D., Wang, H., Feng, X., Chueh, W., Ravikovitch, P., Lyubovsky, M., Takehuchi, T., and Haller, G. L., *J. Phys. Chem.* **103**, 2113 (1999).
11. Zhang, W., Wang, J., Tanev, P. T., and Pinnavaia, T. J., *Chem. Commun.* 979 (1996).
12. Chen, Y.-W., and Lu, Y.-H., *Ind. Eng. Chem. Res.* **38**, 1893 (1999).
13. Wei, D., Chueh, W., and Haller, G. L., *Catal. Today* **51**, 501 (1999).
14. Lim, S., and Haller, G. L., *Appl. Catal. A* **188**, 277 (1999).
15. Berndt, H., Martin, A., Bruckner, A., Schreier, E., Muller, D., Kosslick, H., Wolf, G.-U., and Lucke, B., *J. Catal.* **191**, 384 (2000).
16. Luan, Z., Meloni, P. A., Czernuszewicz, R. S., and Kevan, L., *J. Phys. Chem. B* **101**, 9046 (1997).
17. Neumann, R., and Khenkin, A. M., *Chem. Commun.* 2643 (1996).
18. Oldroyd, R. D., Sankar, G., Thomas, J. M., Hunnius, M., Maier, W. F., *J. Chem. Soc. Faraday Trans.* **94**, 3177 (1998).
19. Wang, Y., Zhang, Q., Ohishi, Y., Shishido, T., and Takehira, K., *Catal. Lett.* **72**, 215 (2001).
20. Beck, J. S., Vartuli, J. C., Roth, W. J., Leonowicz, M. E., Kresge, C. T., Schmitt, K. D., Chu, C. T.-W., Olson, D. H., Sheppard, E. W., McCullen, S. B., Higgins, J. B., and Schlenker, J. L., *J. Am. Chem. Soc.* **114**, 10834 (1992).
21. Dutoit, D. C. M., Schneider, M., Fabrizioli, P., and Baiker, A., *Chem. Mater.* **8**, 734 (1996).
22. Wang, C.-B., Deo, G., and Wachs, I. E., *J. Catal.* **178**, 640 (1998).
23. Yamamoto, T., Tanaka, T., Funabiki, T., and Yoshida, S., *J. Phys. Chem. B* **102**, 5830 (1998).
24. Yamamoto, T., Tanaka, T., Inagaki, S., Funabiki, T., and Yoshida, S., *J. Phys. Chem. B* **103**, 6450 (1999).
25. Concepción, P., López Nieto, J. M., Mifsud, A., and Pérez-Pariente, J., *Appl. Catal. A* **151**, 373 (1997).